

Acquisition of Multiple Real-Time Images for Laser Scanning Microscopy

Michael J. Sanderson, Department of Physiology, Univ of Massachusetts Medical School, Worcester, MA, USA

BIOGRAPHY

Mike Sanderson received his PhD from the Biology Department, University of Southampton, UK, and has been applying imaging techniques to investigate cell physiology. He constructed a high-speed and fluorescence imaging system to measure airway ciliary motion and changes in intracellular calcium. More recently, he has investigated the cell activity within lung slices with self-built confocal and two-photon microscopes.



ABSTRACT

To acquire real-time images from a confocal or 2-photon microscope, a resonant scanning mirror is used to generate the necessary fast horizontal laser scan line. Because the rotational velocity of this mirror is not linear but sinusoidal, it introduces distortion into an image that is acquired by digitization with a constant pixel clock. A correction algorithm based on the phase motion of the mirror removes this distortion and supports a distortion-free zoom capability to the microscope. In real-time, four separate images can be simultaneously acquired, corrected and recorded for extended periods to hard drive.

KEYWORDS

laser-scanning microscopy, image acquisition, real-time, software, frame grabber, zoom control.

ACKNOWLEDGEMENTS

I thank Dr James Sneyd for deriving the correction factor from my calculations and Dr Ian Parker for the confocal microscope design and extensive discussion and advice.

AUTHOR DETAILS

Michael J. Sanderson PhD, Department of Physiology, University of Massachusetts Medical School, 55 Lake Ave North, Worcester, MA 01655, USA.
Tel: +1 508 856 6024
Email: Michael.Sanderson@umassmed.edu
<http://users.umassmed.edu/michael.sanderson/mjslab/>

Microscopy and Analysis, 18 (4): 17-23 (UK), 2004.

INTRODUCTION

Confocal and two-photon microscopy have enhanced the vision of biomedical researchers by providing clearer fluorescence images. The simple premise underlying these techniques is that image contrast is increased by the removal of out-of-focus fluorescent light. In the confocal microscope, out-of-focus light is prevented from reaching the detector by a small aperture that is confocal with the illumination source. By contrast, the two-photon microscope does not require an aperture because there is little out-of-focus light; fluorescence is only generated in a narrow optical plane where the intensity of the laser beam is sufficiently high to allow the simultaneous absorption of two-photons by the fluorophore.

While the resolution and versatility of these microscopes make them a preferred choice for individual research workstations, the cost of commercial systems generally precludes this option. However, a solution can be found with the construction of a home-built laser-scanning microscope. At first sight, this may appear to be a task reserved for a specialist, but surprisingly, it is relatively straightforward. The instructions and parts list required to build a video-rate, laser-scanning confocal microscope have been published [1, 2]. Furthermore, because the two-photon microscope does not require an aperture or descanning optics, the confocal microscope design is easily adapted for a two-photon microscope [3]; the major limiting factor being the cost of the Ti:sapphire laser.

A key principle in generating confocal or two-photon images is the generation of a 2D raster scan across the specimen from a point excitation source (laser). Commonly, a raster scan is generated by reflection from two moving mirrors, aligned at 90° (Fig 1) with the motion of each mirror being driven by a linear saw-tooth control signal. The side-to-side rotation of one mirror creates the horizontal scan line while the up-down rotation of the second mirror creates the vertical deflection. Ideally, throughout the raster scan, the laser beam should remain in the same position on each mirror and this can be achieved by using two concave mirrors to focus the light reflected from one scan mirror on to the next scan mirror [4]. Because this design is difficult for home construction, a compromise that does not appear to significantly reduce image quality is to omit the stationary concave mirrors and mount the vertical deflection mirror on an extension arm (Fig 1). Here, the vertical mirror changes both its position and angle and this

minimizes laser movement on the horizontal deflection mirror [2, 5].

RESONANT SCANNING MIRRORS

A common expectation for microscopy is that image collection should occur quickly. However to attain 30 frames per second (fps), the horizontal scan must move very rapidly (~60 μ s per line, assuming 512 lines per image) and the scan should reposition to the start of the line in less than 3 μ s. While such scanning schemes are possible with electronic systems, inertia limits mechanical scanning systems because mirrors cannot accurately follow rapidly changing saw-tooth control signals. Consequently, a compromise used to attain fast scanning is the substitution of the horizontal linear scanning mirror with a resonant scanning mirror; a mirror that oscillates with a sinusoidal motion (Counter Rotation Scanning Mirror, CRS, General Scanning Inc, MA). The advantage of using this mirror is that it gradually accelerates and decelerates as it progresses through its oscillatory cycle. This avoids the need to rapidly reset the scan to the beginning of each line and a scanning scheme of simply moving from one side to the other can be adopted. To achieve 30 fps, the resonant frequency is tuned to 7.895 kHz (~8 kHz) providing a forward and backward scan cycle in 127 μ s (Fig 1).

IMAGE DISTORTION

One disadvantage of using a resonant scanning mirror is that it introduces distortion into an image that is acquired using a pixel clock operating at a fixed frequency. This approach assumes that the location of the laser is changing linearly, but with a resonant mirror, the position of the laser is changing with a sinusoidal motion. As a result, the image obtained is stretched progressively towards the edges (Fig 2).

Another problem that can result from the slowing velocity of the excitation beam and the associated increase in exposure time of the specimen towards the edges of image area, is that of photobleaching or photodamage. These effects can be minimized by using an aperture with adjustable knife-blade edges to limit the area of exposure. This also has the effect of limiting data collection to the central region of the image where the mirror velocity is approximately linear.

IMAGE CORRECTION

Fortunately, the image distortion induced by the resonant mirror is predictable and cor-

rectable. Although, the resonant mirror only rotates through a small angle ($< 24^\circ$), there is a constant relationship between the angular motion (θ) of the mirror and the periodic motion or phase (ϕ) of the mirror (Figs 1 and 2b). As a result, it is simpler to consider the mirror velocity in terms of phase. At the beginning of the oscillation or scan, the mirror is instantaneously stationary (velocity = 0, phase = $-\pi/2$). As the mirror moves towards the midpoint, its angular velocity increases as a cosine function of the phase. At the middle of the forward scan (phase = 0), the mirror is moving at its fastest (scaled velocity = 1). As the mirror approaches the end of the forward scan ($\pi/2$), its velocity decreases back to 0 (Figs 1 and 2b). The same changes in angular velocity occur as the mirror rotates in the reverse direction.

One approach that has been used to avoid image distortion involves the generation of a pixel clock that has a varying period and reflects the non-linear motion of the excitation beam. A separate laser beam or a portion of the excitation laser beam is directed through a Ronchi grating that consists of equally spaced opaque bars. Because of the varying beam velocity, the time taken for the laser to cross each bar varies and this determines the clock period [6, 7]. This approach is relatively difficult to design and build.

On the other hand, advances with computer technology now make it possible to use all of the image data by performing a rapid correction based on the predictable motion of the mirror. A simple look-up table operating within a software package called Video Savant (IO Industries, Canada) relocates the pixel locations of incoming data to remove image distortion in real-time and record the images to hard disk. The details of how to determine and implement this correction algorithm are provided in Appendix 1. While this correction will work with or without knife-blade edges, it cannot compensate for photobleaching.

ZOOM CONTROL

In addition to the implementation of fast imaging, the use of a scanning resonant mirror has another major benefit of zoom control (Fig 3). This is particularly useful, because it allows the user to adjust the image magnification according to the specimen area without changing objectives. The basis for zoom control is provided by the ability to change the physical angle of the rotation of both the resonant scanning mirror as well as the vertical scanning mirror. A wider scan line, equivalent to a larger angle, reduces the magnification. However, the phase motion of the mirror remains constant and always completes a full scan in 2π . Consequently the same correction algorithm based on the mirror phase continues to function at all zoom positions (Fig 3). Because the saw-tooth waveform driving the vertical mirror is not centered about zero, an offset control is required to re-center the image during zooming. The zoom capability allows the image width to be changed over a factor of ~ 10 (image width 100 to 10 μm). A zoom control is difficult in systems that use the

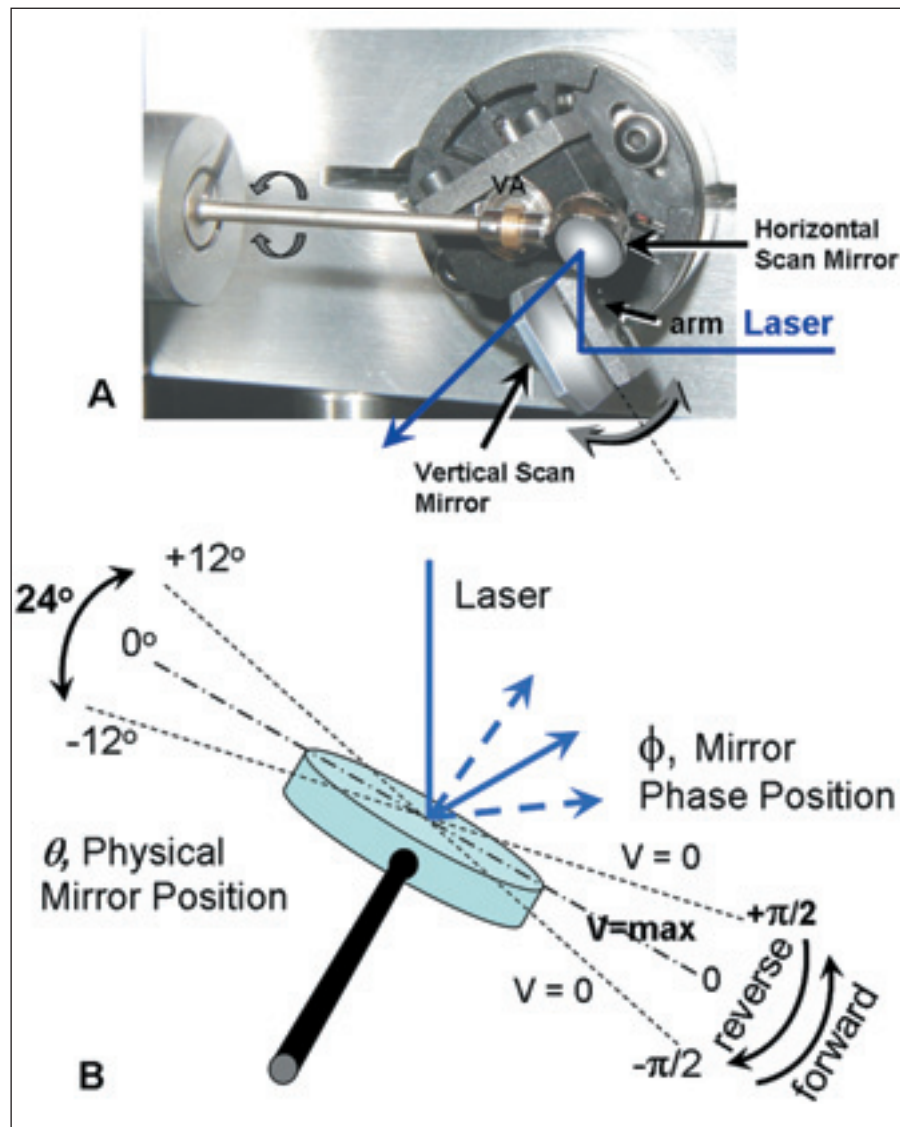


Figure 1:

(A) The orthogonal mechanical arrangement of the resonant scanning mirror that generates a horizontal scan line and the vertical mirror that generates the vertical scan. The horizontal scan mirror rotates forwards and backwards about its axis (circular arrows) while the vertical scan mirror is attached to its rotational axis (VA) by an extension arm (arm-arrow) and moves in the direction of the double-headed arrow. The laser (blue line) strikes each mirror in turn to generate the 2-d raster pattern.

(B) A diagram representing the motion of the resonant horizontal scanning mirror. The mirror can oscillate up to 12 degrees in each direction around its central axis. The laser strikes the surface of the mirror and is reflected according to the rotation. The motion of the mirror can also be considered in terms of the phase of the oscillating cycle. The mirror moves from a phase position (ϕ) of $-\pi/2$ to $+\pi/2$ with the mirror velocity (V) changing from 0 at the beginning of the oscillation to a maximum at the middle of the oscillation.

excitation beam to determine the pixel clock because the laser will either extend past the end of the Ronchi grating at wide scan angles or the pixel resolution will be inadequate at small scan angles.

SIMULTANEOUS COLLECTION OF MULTIPLE CORRECTED IMAGES

While the fast acquisition of corrected images at any zoom factor provides the scanning microscope with a basic configuration, another desirable feature for a microscope system is the ability to excite and detect the fluorescence from different fluorophores simultaneously. In addition, a transmitted light image is useful to correlate structures with fluorescence. The separation of the appropriate wavelengths to examine different images,

based on the use of dichroic beam splitters and barrier filters, is a standard practice. However, the collection of multiple images at 30 fps requires extremely rapid data acquisition, correction and storage.

A solution to this problem has been achieved using a digital framegrabber (The Raven) from Bit Flow, Inc. This framegrabber has the ability to simultaneously digitize inputs from four sources at 30 fps. The same vertical and horizontal synchronization signals are used for all sources. While computer memory can be used for image storage, its capacity is limited and can be quickly exceeded with two or more acquisition channels. It is therefore more appropriate to record images directly to computer hard drive and this is achieved with the software Video Savant. The software acts as an interface between the

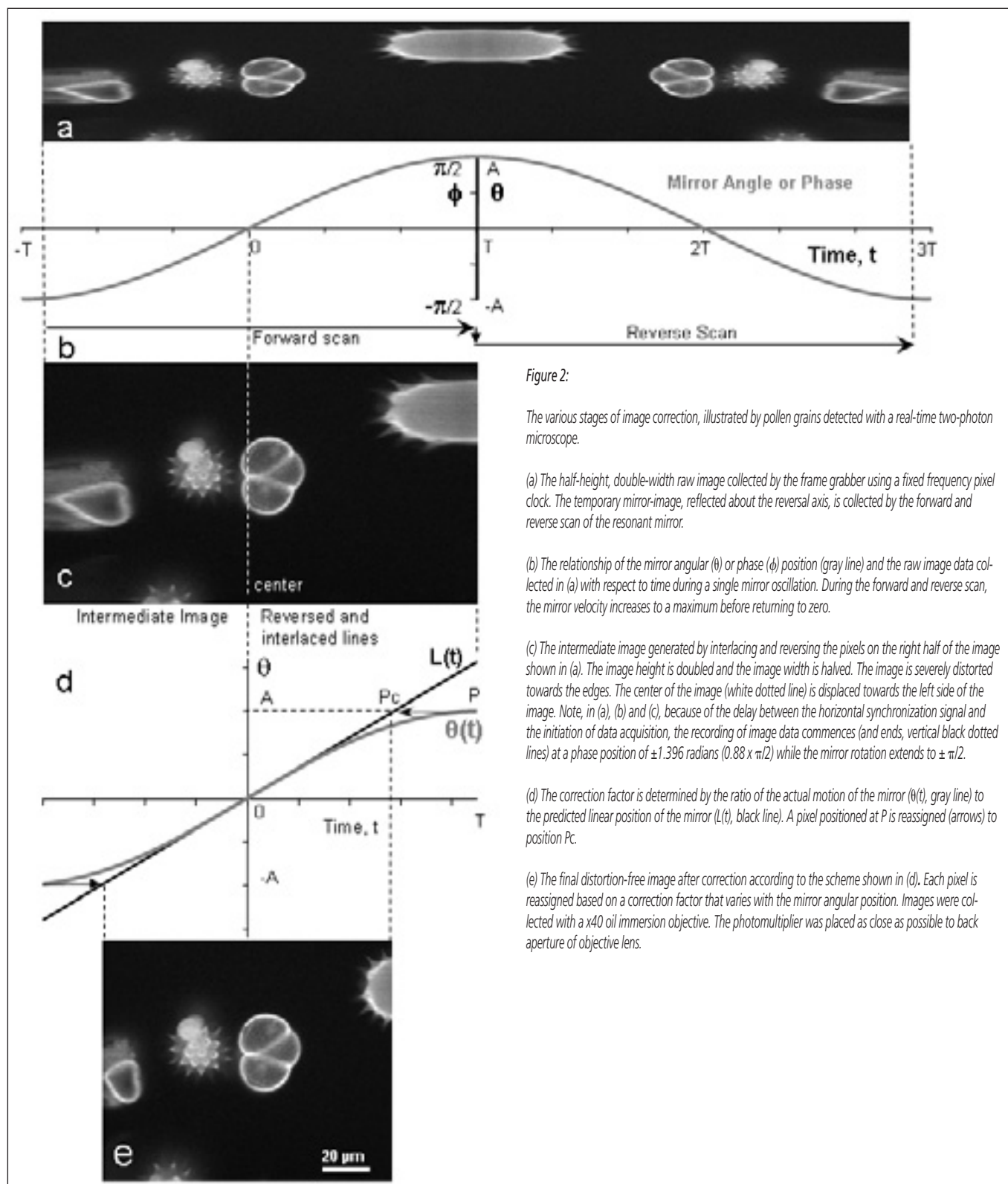


Figure 2:

The various stages of image correction, illustrated by pollen grains detected with a real-time two-photon microscope.

(a) The half-height, double-width raw image collected by the frame grabber using a fixed frequency pixel clock. The temporary mirror-image, reflected about the reversal axis, is collected by the forward and reverse scan of the resonant mirror.

(b) The relationship of the mirror angular (θ) or phase (ϕ) position (gray line) and the raw image data collected in (a) with respect to time during a single mirror oscillation. During the forward and reverse scan, the mirror velocity increases to a maximum before returning to zero.

(c) The intermediate image generated by interlacing and reversing the pixels on the right half of the image shown in (a). The image height is doubled and the image width is halved. The image is severely distorted towards the edges. The center of the image (white dotted line) is displaced towards the left side of the image. Note, in (a), (b) and (c), because of the delay between the horizontal synchronization signal and the initiation of data acquisition, the recording of image data commences (and ends, vertical black dotted lines) at a phase position of ± 1.396 radians ($0.88 \times \pi/2$) while the mirror rotation extends to $\pm \pi/2$.

(d) The correction factor is determined by the ratio of the actual motion of the mirror ($\theta(t)$, gray line) to the predicted linear position of the mirror ($L(t)$, black line). A pixel positioned at P is reassigned (arrows) to position P_c .

(e) The final distortion-free image after correction according to the scheme shown in (d). Each pixel is reassigned based on a correction factor that varies with the mirror angular position. Images were collected with a $\times 40$ oil immersion objective. The photomultiplier was placed as close as possible to back aperture of objective lens.

frame grabber and a striped volume set of SCSI hard drives within the computer. The correction look-up table is applied to all four channels without a loss of speed. With multiple fast SCSI drives, a recording rate of about 120 MB per second can be achieved. This is more than adequate to record 120 fps (4 channels at 30 fps each). The numbers of images that can be captured is only limited by the size of the hard drive (~ 120 GB). In addition to recording the images, it is often desirable to overlay each image to understand the spatial relationship

of the emitted fluorescence. Video Savant software can combine and overlay 3 different channels in pseudocolor while also displaying the original images.

FRAME RATE AND IMAGE RESOLUTION

It is unlikely that a single set of image acquisition parameters will be appropriate for all applications and in this respect the design using a resonant scanning mirror shows considerable versatility. While the scan rate of the

horizontal line is fixed by the resonant period, the number of lines collected per image can be varied. For example, if half the number of lines are collected, frame rate is doubled (i.e. 30 fps at 400 lines or 60 fps at ~ 180 lines, some additional lines are lost due to the repositioning of the vertical mirror). Alternatively, a single line can be collected for a line-scanning mode ($63.5 \mu\text{s}/\text{line}$). Image resolution can also be increased by increasing the number of pixels per line by increasing the pixel clock to 15 MHz. However, it is always important to maintain a square

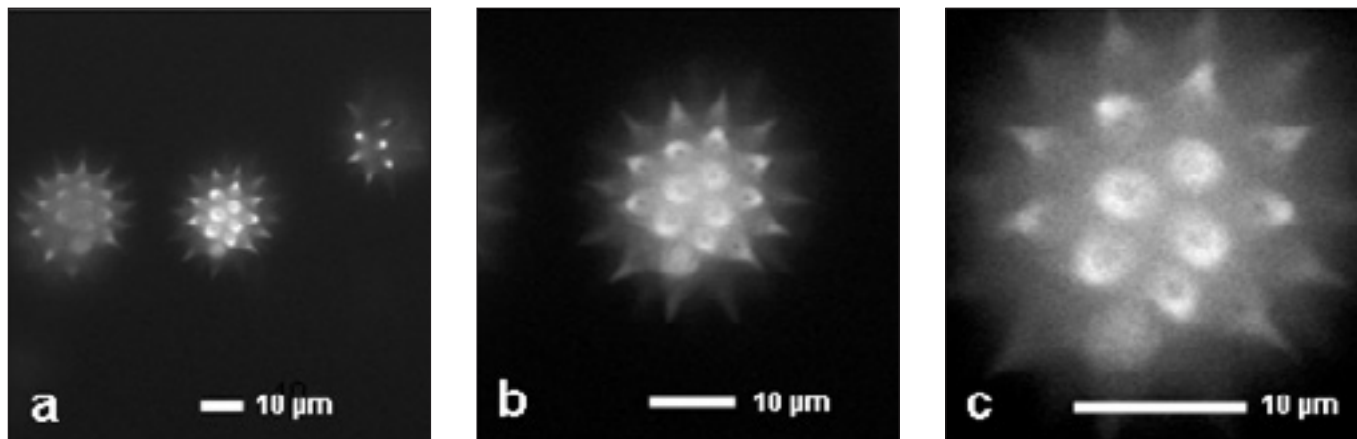


Figure 3: Three images of a same pollen grain taken with a two-photon microscope using a x40 oil, 1.3 NA objective. By decreasing (a through c) the scan angle of the horizontal and vertical scan mirrors, a zoom effect is achieved (a x1, b x2, c x4). The same correction algorithm was used at all zoom positions to remove image distortion. Final images are average of 4 raw images.

aspect ratio for each pixel. This is achieved by calibrating the width and height of the image over the range of the zoom control for both the vertical and horizontal scans and by determining the image aspect ratio by examining a square grid provided by a stage micrometer. To offset the decrease in the vertical distance viewable with the higher horizontal resolution, an increase in the number of horizontal lines per image may be desirable. With the current design, the numbers of lines per image is easily changed by a factor of 2 (400 to 800).

CONCLUSION

While the use of a resonant scanning mirror provides a versatile approach to laser scanning microscopy, its non-linear motion introduces image distortion. However, the predictable sinusoidal motion of the mirror allows for the construction of a simple image correction algorithm that operates in real-time. This coupled with a four-channel framegrabber (The Raven) and fast digital-image recording software (Video Savant) provides the ability to rapidly record multiple, distortion-free confocal or two-photon microscopy images directly to hard drive.

APPENDIX 1: CORRECTION ALGORITHM

DATA COLLECTION

Pixel data are collected as the resonant mirror scans in both the forward and reverse direction. In order not to trace over the same line, the control electronics advance the vertical scan position by one line at the beginning of the forward and reverse scan. In our design, only one horizontal line synchronization pulse (forward scan) is delivered to the framegrabber. The pixel data are stored as if they originated from a single line and a temporary image created in memory is twice the final image width and half the final image height (Fig 2a).

IMAGE RECONSTRUCTION

The first step in producing the final image is

the reversal of the order of the data points from the second half of the line, and the interlacing of this reversed data between the data lines of first the half of the image (Fig 2c). The rearrangement of the pixel data requires that the mirror reversal point within the image is known. This location may not be the mid-point of the temporary image because the precise relationship between the position of the resonant mirror and the horizontal synchronization signal that triggers the acquisition of each line can be difficult to determine. Depending on the framegrabber, a few to tens of pixel-clock pulses can elapse before synchronization of the data acquisition is established (Fig 2b). Consequently, the pixel width of the image will often not equal the number of pixel-clock pulses per line. However, an easy solution to finding the reversal point lies within the viewed image. If the image data are reversed and interlaced around the wrong pixel, a double image is revealed with each image being slightly out of register. By using Video Savant software to offset one image with respect to the other, the images can be interactively aligned (Fig 2c). When a single image is formed, the right edge of the image is the reversal point of the resonant scanning mirror (phase = $+\pi/2$) (Fig 2c) and serves as a fundamental reference point for the image.

IMAGE CORRECTION

This consists of four basic steps: i) determining a phase constant for the mirror and frame grabber; ii) determining the center pixel of the final image; iii) determining the correction factor for each pixel or phase position relative to the center pixel; and iv) relocating the pixel position as indicated by the correction factor.

Phase constant

The phase constant ($\Delta\phi$), defined as the change in phase position per clock cycle is determined by:

$$\Delta\phi = 2\pi / n$$

and $n = p \times f$

where n equals the number of pixels per line,

p equals the period of the scan line (μs) and f equals the frequency of the pixel clock (MHz). For our configuration, the period of the line scan is determined by the resonant frequency of the mirror (the 8 kHz model has 7875 lines/sec, a line period of 127 μs) and we have set the framegrabber (Raven Board) pixel clock at 12 MHz.

Image center pixel

The center of the final image is located at the position where the mirror has moved through a 1/4 of its cycle. Thus:

$$\text{center pixel} = n / 4$$

However, care must be used to express the value of this pixel from the right-edge of the image where the exact phase position of the mirror is known ($\pi/2$ {right edge} to 0 {image center}) and not from the left-edge where image data may not be available.

Correction factor

The correction factor (C) varies with the mirror phase and is calculated from the phase constant, $\Delta\phi$, and the pixel location relative to the center pixel of the image (redefined to equal 0) where the mirror phase is = 0. Thus

$$\phi = \Delta\phi \times \text{pixel number,}$$

and

$$C = \frac{\phi}{\sin \phi}$$

The derivation of the correction factor is detailed in Appendix 2.

Pixel relocation

Again, proceeding outwards from the center pixel location (0),
New pixel position = (old pixel position / C)

The old and new pixel locations are incorporated into a look-up table that is used to reassign the pixel locations as they are captured. Approaching the center of the image, the correction factor approaches 1.0 and the pixel

locations change little. Approaching the edges of the image the correction factor approaches $\pi/2$ and pixels are relocated closer to the image center (Figs 2d and 2e). Because pixel locations are discrete physical elements they can only exist as integer values and the result of the relocation algorithm must be rounded to the nearest pixel value. As a result, several adjacent pixels are re-assigned to the same new location. The duplicate pixels are discarded with the result that the image width is decreased.

APPENDIX 2: DERIVATION OF THE CORRECTION FACTOR, C

θ denotes the physical rotational angle of the resonant scanning mirror (Figs 1, 2b and 2d), and θ varies as a sine function of time. If the mirror takes a time $2T$ to rotate from the angle $-A$ to the angle A (where T can take any positive value, and A can take any positive value less than or equal to 90 degrees), we can express θ as a specific function of time:

$$\theta(t) = A \sin\left(\frac{\pi t}{2T}\right)$$

as shown in Fig 2b. The angular velocity of the mirror is the derivative of the above function. Consequently, when the mirror is moving the fastest, i.e. when its physical angle is 0, (Fig 2d) the maximal angular velocity of the mirror is:

$$\theta'(0) = \frac{\pi}{2T} A \cos\left(\frac{\pi \cdot 0}{2T}\right) = \frac{\pi A}{2T}$$

Referring to Fig 2d, the line labeled $L(t)$ is tangent to the curve $\theta(t)$ at $t=0$, and thus $L(t)$ is described by the equation

$$L(t) = \frac{\pi A}{2T} t$$

At any time, we define the correction factor as the ratio between the curve $\theta(t)$ (where the measurement point really is) and the curve $L(t)$ (where the pixel clock predicts the measurement is). Hence:

$$\text{correction}(t) = \frac{L(t)}{\theta(t)} = \frac{(\pi A/2T)t}{A \sin(\pi t/2T)} = \frac{(\pi t/2T)}{\sin(\pi t/2T)}$$

Finally, we notice that $\frac{\pi t}{2T}$, which we shall call

ϕ , is the phase of the mirror cycle (expressed in radians). In other words, when $t = -T$, $\phi = -\pi/2$ and when $t = T$, $\phi = \pi/2$. Using the phase of the mirror rather than the time to express the correction factor gives a simpler expression for the correction factor (C) as

$$C = \frac{\phi}{\sin(\phi)}$$

Note that, as the phase approaches zero, i.e. as the mirror is moving fastest, the correction factor approaches one, while the correction factor is largest as the phase approaches $\pm \pi/2$. The correction factor is also independent of the physical angle of the mirror A .

REFERENCES

1. Sanderson, M.J. and I. Parker, Video-rate confocal microscopy. *Methods Enzymol*, 2003. 360: p. 447-81.
2. Callamaras, N. and I. Parker, Construction of a confocal microscope for real-time x-y and x-z imaging. *Cell Calcium*, 1999. 26(6): p. 271-9.
3. Nguyen, Q.T., et al., Construction of a two-photon microscope for video-rate Ca(2+) imaging. *Cell Calcium*, 2001. 30(6): p. 383-93.
4. Amos, W.B. and J.G. White, How the confocal laser scanning microscope entered biological research. *Biol Cell*, 2003. 95(6): p. 335-42.
5. Stelzer, E., The intermediate optical systems of laser-scanning confocal microscopes, in *Handbook of confocal microscopy*, J.B. Pawley, Editor. 1995, Plenum: New York. p. 139 - 154.
6. Fan, G.Y., et al., Video-rate scanning two-photon excitation fluorescence microscopy and ratio imaging with cameleons. *Biophys J*, 1999. 76(5): p. 2412-20.
7. Tsien, R. and B.J. Bacski, Video-rate confocal microscopy, in *Handbook of biological confocal microscopy*, J.B. Pawley, Editor. 1995, Plenum Press: New York. p. 459 - 478.

©2004 John Wiley & Sons Ltd